Influence of optical aberrations on laser-induced plasma formation in water and their consequences for intraocular photodisruption

Alfred Vogel, Kester Nahen, Dirk Theisen, Reginald Birngruber, Robert J. Thomas, and Benjamin A. Rockwell

The influence of spherical aberrations on laser-induced plasma formation in water by 6-ns Nd:YAG laser pulses was investigated for focusing angles that are used in intraocular microsurgery. Waveform distortions of 5.5λ and 18.5λ between the optical axis and the $1/e^2$ irradiance values of the laser beam were introduced by replacement of laser achromats in the delivery system by planoconvex lenses. Aberrations of 18.5λ increased the energy threshold for plasma formation by a factor of 8.5 compared with the optimized system. The actual irradiance threshold for optical breakdown was determined from the threshold energy in the optimized system and the spot size measured with a knife-edge technique. For aberrations of 18.5λ the irradiance threshold was 48 times larger than the actual threshold when it was calculated by use of the diffraction-limited spot size but was 35 times smaller when it was calculated by use of the measured spot size. The latter discrepancy is probably due to hot spots in the focal region of the aberrated laser beam. Hence the determination of the optical-breakdown threshold in the presence of aberrations leads to highly erroneous results. In the presence of aberrations the plasmas are as much as 3 times longer and the transmitted energy is 17–20 times higher than without aberrations. Aberrations can thus strongly compromise the precision and the safety of intraocular microsurgery. They can further account for a major part of the differences in the breakdown-threshold and the plasma-transmission values reported in previous investigations.

OCIS codes: 140.3440, 170.4470, 220.1010, 350.3390, 350.5400.

1. Introduction

Laser-induced plasma formation (optical breakdown) in water or aqueous fluids is used in various medical laser applications,[1,2] such as laser lithotripsy,[2] laser angioplasty,[3] and intraocular microsurgery.[2,4–6] Additionally, laser-induced breakdown is of great importance in the field of laser safety, as it is a possible mechanism for ocular damage by short and ultrashort laser pulses.[7]

Theoretical investigations of laser-induced plasma formation usually are based on the assumption of diffraction-limited focusing. In previous experimental investigations of optical-breakdown phenomena, we also attempted to realize such conditions to guarantee reproducability and to facilitate comparison with theory.[8–10] In many practical laser applications, however, the laser focus deteriorates because of aberrations. This is the case, for example, in intraocular microsurgery, especially when the application site is located in the ocular periphery, where an oblique passage of the laser beam through the ocular media and the crystalline lens is unavoidable.[4] Similar considerations apply for laser-induced retinal damage because the retinal image is influenced by the aberrations of the eye.[11–15] Aberrations change the irradiance distribution in the region of the laser focus and thus alter the breakdown threshold, the plasma form, and the plasma length. These alterations may lead to changes of the plasma transmission and to differences in the conversion of light energy to the mechanical energy of the shock wave and of the cavitation bubble, which are created by the expanding plasma. These phenomena influence the precision of intraocular photodisruption[6,10] and may also affect the characteristics and the severity of oc-

A. Vogel (vogel@mll.mu-lubeck.de), K. Nahen, D. Theisen, and R. Birngruber are with the Medical Laser Center Lübeck, Peter-Monnik Weg 4, D-23562 Lübeck, Germany. R. J. Thomas and B. A. Rockwell are with the Air Force Research Laboratory, 8111 18th Street, Brooks Air Force Base, Texas 78235-5215.

Received 3 August 1998; revised manuscript received 23 February 1999.
0003-6935/99/163636-08$15.00/0

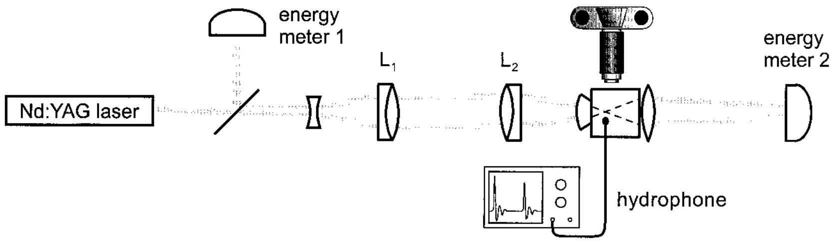

Fig. 1. Experimental arrangement for the investigation of plasma formation. For introducing spherical aberrations of different degrees, achromats L_1 and L_2 were replaced by planoconvex lenses.

ular damage occurring in a laser accident. They are investigated in this study to complete earlier research performed with minimized aberrations.[9,10]

Besides having practical importance for intraocular photodisruption and laser safety, a study of the effects of aberrations on optical breakdown might also explain some of the discrepancies between previous studies on optical-breakdown thresholds and plasma shielding in aqueous media.[8–10,16–26] The assumption of diffraction-limited focusing conditions in the presence of optical aberrations leads to erroneous conclusions about the physics of optical breakdown. The breakdown-irradiance threshold I_{th} is overestimated, and, because the aberrations tend to be more pronounced at large focusing angles (small spot sizes), an apparent dependence of the breakdown threshold on spot size is created.[9,27,28] Even if the aberrations of the delivery system are minimized in air the liquid cell introduces additional aberrations if simple cuvettes with plane walls are used.[29] A way to avoid these problems is to build suitable lenses into the cuvette wall, for example, aplanatic meniscus lenses.[8,9,16] In this case, however, great care has to be taken that the focus is located in the aplanatic point of the lens. If the focus is located behind the aplanatic point strong spherical aberrations are created.[30]

Few researchers have taken all the above-described precautions into account in their investigations of optical breakdown in liquids. Hence the measurement results were often influenced by aberrations, but, because the experimental conditions frequently were not well documented, it is difficult to assess to what degree. The present investigation shows the wide range in which optical-breakdown phenomena vary when the quality of the laser focus is changed by aberrations.

The parameter range that we investigated covers the parameters used for intraocular microsurgery. The delivery system for the laser pulses was first optimized to achieve minimal aberrations; then known spherical aberrations were introduced by the replacement of achromatic laser doublets by simple planoconvex lenses. The breakdown phenomena that were investigated include the optical-breakdown threshold, the plasma shape and length, the plasma transmission, and the conversion of light energy into mechanical energy.

2. Methods

The experimental arrangement for investigation of the influence of aberrations on plasma formation is shown in Fig. 1. The optical system for plasma generation is described in detail in Ref. 9 and therefore is summarized only briefly here. All experiments were performed with Nd:YAG laser pulses having a duration of 6 ns and a nearly Gaussian intensity profile. When minimal aberrations were desired the laser beam was expanded by a biconcave lens ($f = -40$ mm), collimated by a Nd:YAG laser achromat L_1 ($f_1 = 200$ mm), and focused into a cuvette filled with distilled filtered water by use of a second laser achromat L_2 ($f_2 = 120$ mm). An ophthalmic contact lens (Rodenstock, Model RYM) was built into the cuvette wall, and the laser focus coincided with the aplanatic point of the contact lens. The focusing angle was 22°, and the focus diameter was 7.6 μm (the diffraction-limited spot diameter was 3.5 μm).

Spot-size measurements were performed by use of a knife-edge technique.[9,31] The laser-pulse energy was kept low enough to avoid plasma formation at the knife edge. The beam radius was determined in various planes in the region of the beam waist, as described in Ref. 31. We measured at which knife-edge positions 10% and 90% of the maximum pulse energy were transmitted and calculated the beam radius ω at the $1/e^2$ irradiance values under the assumption of a Gaussian beam profile. (The latter assumption is not correct for aberrated laser beams, but we wanted to use the same technique for all measurements.) Beam propagation in the focal region is given by[32]

$$\omega(z) = \omega_0 \left[1 + \left(\frac{M^2 \lambda z}{\pi {\omega_0}^2} \right)^2 \right]^{1/2}, \tag{1}$$

where $2\omega_0$ is the spot diameter, $\omega(z)$ is the beam radius at location z along the optical axis, and M is a parameter describing the quality of the beam. Equation (1) was fitted to the measurement data for $\omega(z)$ to obtain ω_0.

To introduce known aberrations, we replaced the achromats L_1 and L_2 with planoconvex lenses (achromatic doublets minimize not only chromatic but also spherical aberrations) and used a stronger beam expansion ($f = -30$ mm). The degree of aberration can be described in terms of an aberration function Φ, which is defined as the displacement between the perfectly spherical wave front and the distorted wave front. For a planoconvex lens of focal length f, radius r_0, and refractive index n, the aberration function is given by[33]

$$\Phi(\rho) = -\frac{(r_0\rho)^4}{32f^3}\left[\frac{n^2}{(n-1)^2} - \frac{n}{n+2} + \frac{(2n^2-n-4)^2}{n(n+2)(n-2)^2}\right], \tag{2}$$

where $\rho = r/r_0$ and r represents distances measured orthogonal to the optical axis. The maximum value Φ_{max} of Φ occurs at the beam edge defined by the lens aperture. For a Gaussian intensity distribution the quality of the focus depends not only on Φ_{max} but also on the location r_G of the $1/e^2$ irradiance values relative to the lens aperture. We therefore use $\Phi(r_G)$ to characterize the aberrations of the optical system. Replacing the achromat L_1 with a planoconvex lens with a 200-mm focal length led to $\Phi(r_G) = 5.5\lambda$. We created stronger aberrations of $\Phi(r_G) = 18.5\lambda$ by additionally replacing achromat L_2 with a planoconvex lens with a 150-mm focal length. The corresponding focusing angles were 28° for $\Phi(r_G) = 5.5\lambda$ and 24° for $\Phi(r_G) = 18.5\lambda$. The spot diameters were 96 and 130 μm, respectively. The aberrations investigated in this paper are fairly strong to demonstrate the effects of focal distortions clearly. Aberrations of this degree sometimes occurred in investigations of the physics of photodisruption,[23,27,33] and they may arise (mainly in the form of astigmatisms and coma) during laser treatment in the ocular periphery or in laser accidents in which the beam is incident from an oblique angle.

The energy thresholds E_{th} for optical breakdown (a 50% breakdown probability) were determined by visual detection of the plasma spark, as described in Ref. 9. We also determined the sharpness, $S = E_{th}/\Delta E$, of the threshold, which is given by the ratio of E_{th} to the energy difference ΔE between a 10% and a 90% breakdown probability.[9] The plasma form and length were analyzed with a spatial resolution of approximately 4 μm by open-shutter photography in a darkened room.[9] Plasma transmission was measured by use of calibrated energy detectors in front of and behind the water-filled cuvette (Fig. 1), as described in Ref. 10.

Mechanical effects that arise during the optical-breakdown process are cavitation and shock-wave emission.[34] The bubble energy E_B can be determined easily in an indirect way through a hydrophone measurement of the bubble's oscillation period, which is marked by the shock waves emitted during optical breakdown and bubble collapse.[35] The oscillation period T_B is related to the maximum bubble radius R_{max} by[36]

$$R_{max} = T_B/1.83\left(\frac{\rho_0}{p_\infty - p_v}\right)^{1/2}, \tag{3}$$

Table 1. Breakdown Parameters for Various Degrees of Optical Aberrations

Breakdown Parameters	Spherical Aberrations: Minimized	$\Phi(r_G) = 5.5\lambda$	$\Phi(r_G) = 18.5\lambda$
Focusing angle θ	22°	28°	24°
Spot diameter (μm)			
Diffraction limited	3.5	2.7	3.2
Measured	7.6 ± 0.6	96.6 ± 3.6	130.2 ± 5.9
E_{th} (μJ)	141 ± 1.3	371 ± 3	1202 ± 9
I_{th} ($\times 10^{11}$ W cm^{-2})			
Diffraction limited	2.44	10.8	24.9
Measured	0.52	0.0084	0.015
Sharpness S of threshold	2.05	1.88	1.48

where ρ_0 is the density of the liquid, p_∞ is the hydrostatic pressure, and p_v is the vapor pressure inside the bubble (2330 Pa at 20 °C). The maximum bubble radius, in turn, yields the bubble energy:

$$E_B = (4\pi/3)(p_\infty - p_v)/R_{max}{}^3. \tag{4}$$

The shock-wave energy E_S cannot be determined easily because it depends on the shock-wave amplitude and profile near the plasma, which are difficult to measure.[34] Previous investigations showed, however, that the ratio between the bubble energy and the shock-wave energy is similar for 1-mJ and 10-mJ pulses of 6-ns duration.[34,37] We assume that the ratio is also approximately constant for a wider parameter range and consider the transformation of light energy into bubble energy E_B to be indicative of the conversion of light energy into mechanical energy ($E_B + E_S$).

To support the interpretation of the experimental results, we calculated the light-intensity distribution in the focal region of the laser beam by evaluating the diffraction integral[27]:

$$I(r, z) = \left(\frac{2\pi A_0 r_0{}^2}{\lambda f^2}\right)^2 \left|\int_0^1 \exp(0.5\ \rho^2)\exp\{i[k\Phi(\rho) - 0.5u\rho^2]\}J_0(v\rho)\rho d\rho\right|^2, \tag{5}$$

where $\Phi(\rho)$ is the aberration function given by Eq. (1), $k = 2\pi/\lambda$, A_0 is the incident-beam amplitude, z defines the direction of the optical axis, and u and v are the so-called optical coordinates:

$$u = \frac{2\pi}{\lambda}\left(\frac{r_0}{f}\right)^2 z, \qquad v = \frac{2\pi}{\lambda}\left(\frac{r_0}{f}\right) r.$$

3. Results and Discussion

A. Breakdown Thresholds

The breakdown parameters for various degrees of spherical aberration are summarized in Table 1. For the strongest aberrations investigated [$\Phi(r_G) = 18.5\lambda$] the energy threshold E_{th} is 8.5 times as large

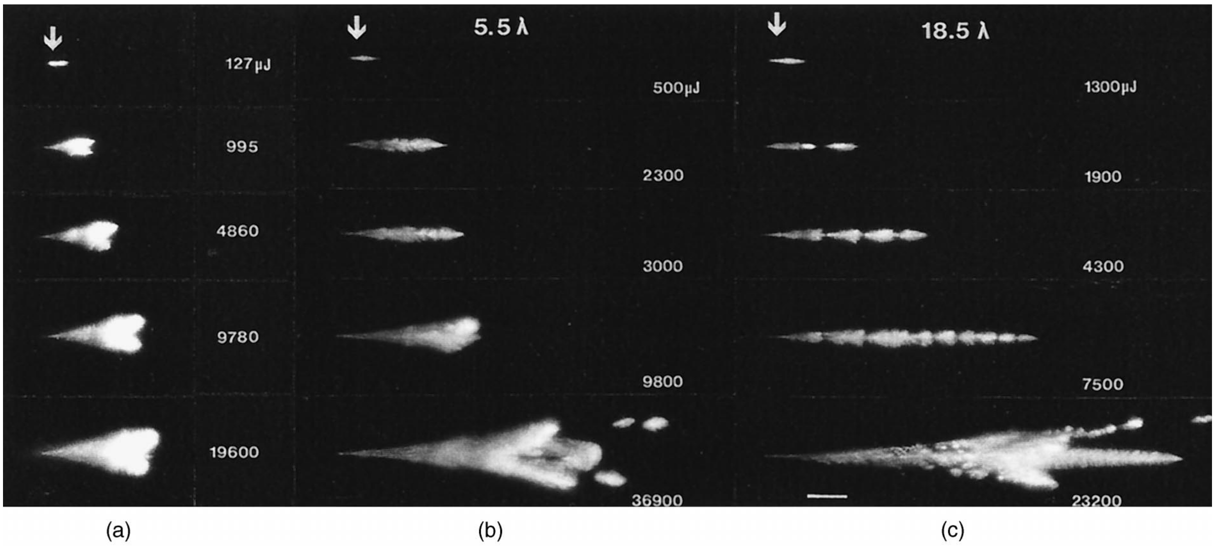

Fig. 2. Plasma shape as a function of laser-pulse energy for various degrees of aberration: (a) minimized aberrations, (b) $\Phi(r_G) = 5.5\lambda$, (c) $\Phi(r_G) = 18.5\lambda$. The laser light is incident from the right. The arrows indicate the locations of the beam waists. The bar represents a length of 100 μm. The pulse energies are given in microjoules.

as for minimized aberrations. The sharpness S of the threshold decreases with an increasing degree of aberration.

The most precise value of the threshold irradiance is obtained when the threshold energy and the spot size measured for the case of minimized aberrations are used for the calculation of I_{th}. For simplicity, we call this value ($I_{\mathrm{th}} = 0.52 \times 10^{11}$ W cm^{-2}) the actual breakdown threshold. Use of the *diffraction-limited* spot size for the calculation of I_{th} leads to erroneously large values, particularly for strong aberrations. The value obtained for $\Phi(r_G) = 18.5\lambda$ is 48 times larger than the actual threshold value. Even in the case of an optimized delivery system the threshold obtained by use of the diffraction-limited spot is still 4.7 times larger than the actual value because residual aberrations are hard to avoid at large focusing angles.

When the *measured* spot size is used to calculate the irradiance threshold for an aberrated beam, one obtains values for I_{th} that are considerably lower than the actual threshold. For $\Phi(r_G) = 18.5\lambda$, the I_{th} value is now 35 times lower than the value obtained with minimum aberrations. This discrepancy is most likely due to the presence of hot spots in the focal region of the aberrated laser beam (see Figs. 2 and 3, below), where plasma formation can start before the breakdown threshold is surpassed in the entire focal volume. In these hot spots, the threshold irradiance is probably the same as in the optimized system, but calculations with the whole measured diameter of the beam waist yield a reduced threshold value because they average over the hot spots and the low-intensity regions. We can conclude that the presence of aberrations leads to erroneous values of the optical-breakdown threshold even when the measured spot size is used for its determination.

B. Plasma Shape

Figure 2 shows how the plasma shape changes because of spherical aberrations. The plasmas produced with minimal aberrations are compact and fill the whole cone angle of the laser beam. Spherical aberrations lead to plasmas that are longer, are less compact, and often consist of several individual parts. They feature a sharp tip in the cone angle beyond the laser focus, and at large pulse energies wings are formed in the periphery of the laser beam.

One can understand the respective plasma shapes by looking at the intensity distribution in the focal region of the laser beam. The plasma shape follows isointensity lines in the cone angle proximal to the laser.[9,38] Figure 3 shows the intensity distribution calculated by evaluation of the diffraction integral in Eq. (4). In the presence of spherical aberrations the peripheral parts of the laser beam are more strongly focused than the central parts. This difference in focus leads to an intersection of the peripheral and the central rays before the beam waist and thus to a zone of high intensity that has the form of a hollow cone. The tip of the conical zone results from the central rays that are focused downstream from the beam waist. Interference phenomena lead to a modulation of this pattern and thus to the formation of hot spots. The region of peak irradiance is small compared with the total size of the beam waist. This relation explains the strong reduction of the threshold value when I_{th} is calculated with the assumption of a homogeneous intensity distribution across the whole measured beam diameter.

The calculated irradiance distributions shown in Fig. 3 closely resemble the experimentally observed plasma shapes shown in Figs. 2(b) and 2(c). At small normalized pulse energies, $\beta = E/E_{\mathrm{th}}$, plasma

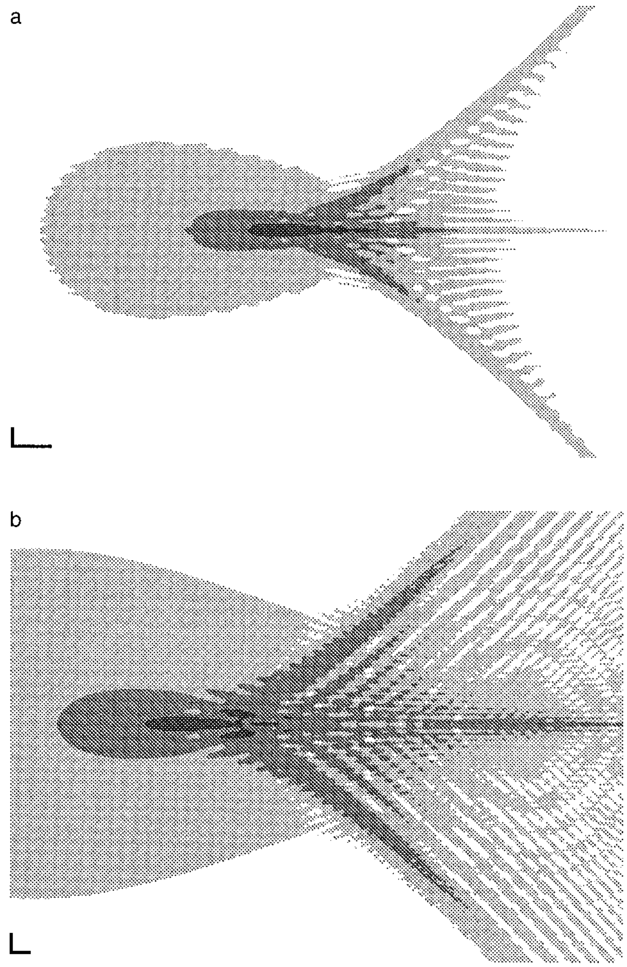

Fig. 3. Calculated intensity distribution in the focal region for (a) $\Phi(r_G) = 5.5\lambda$ and (b) $\Phi(r_G) = 18.5\lambda$. The laser light is incident from the right. The vertical and the horizontal bars represent a length of 10 μm and 100 μm, respectively. The three gray levels represent a total irradiance range of 100:1.

is formed in only the intensity maxima along the optical axis (for example, in the case of $\Phi(r_G) = 18.5\lambda$ and $E = 4300$ μJ, corresponding to $\beta = 3.6$). At larger pulse energies, the individual breakdown sites grow together, and plasma is also produced in the high-intensity wings in the beam periphery. Besides at the tip of the conical high-intensity region, little plasma is produced beyond the beam waist because most of the laser light is absorbed by the plasma proximal to the laser (plasma shielding).[10] Plasma shielding is not visible in Fig. 3 because the influence of plasma absorption on the irradiance distribution in the focal region was not considered in the calculations.

C. Plasma Length

At energies well above the breakdown threshold, the plasmas are as much as 3 times longer in the presence of aberrations (Fig. 4), and the plasma length at threshold also increases slightly with increasing aberrations. The longer length is due to distortions of the plasma form and to individual plasma spots outside the main body of the plasma (Figs. 2 and 3).

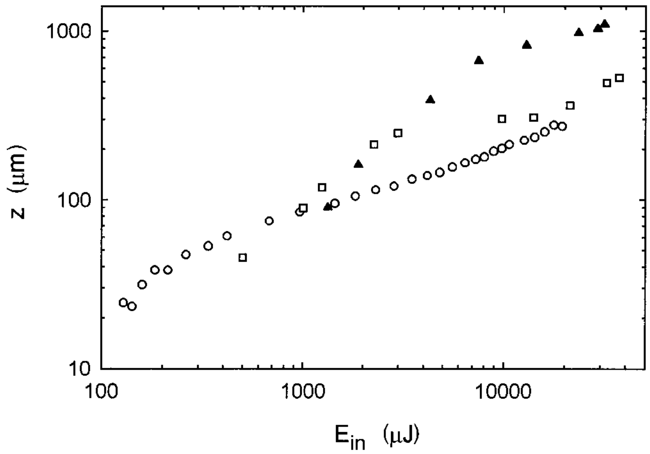

Fig. 4. Plasma length as a function of the laser-pulse energy for minimized aberrations (open circles), $\Phi(r_G) = 5.5\lambda$ (open squares), and $\Phi(r_G) = 18.5\lambda$ (filled triangles).

D. Plasma Transmission

Aberrations lead to a considerable increase in plasma transmission. The transmitted energy is, for $\Phi(r_G) = 18.5\lambda$ in the whole parameter range investigated, 17–20 times higher than in the optimized system (Fig. 5). The increase of transmitted energy is partly due to the higher breakdown threshold resulting from the increased spot size and partly a consequence of the irregular irradiance distribution in the focal region. The incident light is absorbed in the irradiance maxima where plasma is formed but is partially transmitted between and beside the maxima. Therefore a larger percentage of the laser light is transmitted (Fig. 6). The percent transmission at threshold was 50% in the optimized system but 85% with strong aberrations.

Various other authors previously measured the transmission of plasmas created in water and saline by nanosecond Nd:YAG laser pulses[16–18,20–23,26] and reported a wide variety of results. These results cannot be compared in detail with the data of the current study because the medium of plasma formation, the laser beam profile, the focusing angle, and the interface between the liquid cell and air (a plane wall or a lens built into the cell) differ from case to case and sometimes are not even reported. All transmission values reported are, at equal β, larger than the values obtained by us with minimized aberrations, and most values are smaller than our values for $\Phi(r_G) = 18.5\lambda$. This trend suggests that optical aberrations in the delivery system of the laser pulses can account for a major part of the differences in transmission values obtained by different authors.

E. Conversion of Light Energy into Cavitation-Bubble Energy

Figure 7 shows that the conversion rate of laser-light energy E_L into cavitation-bubble energy E_B decreases

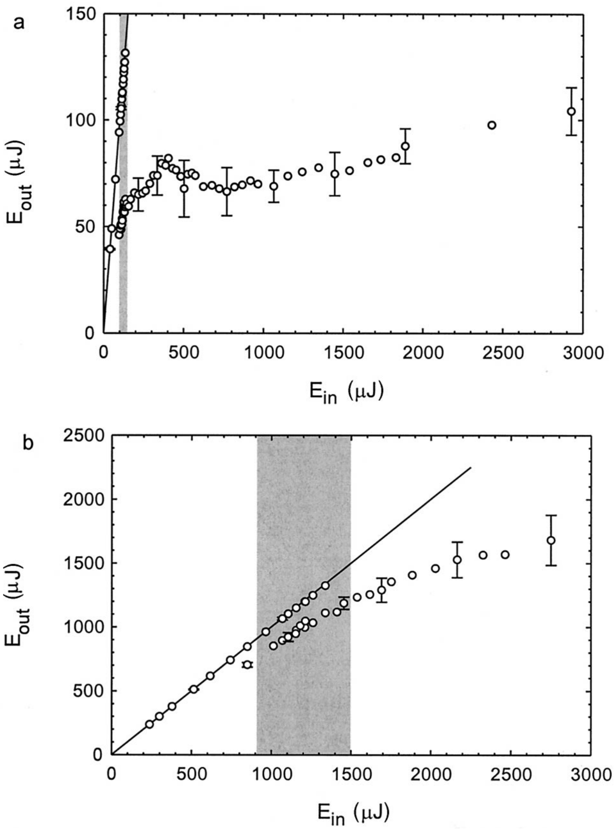

Fig. 5. Transmitted energy as a function of the incident laser energy for (a) minimized aberrations and (b) $\Phi(r_G) = 18.5\lambda$. The shaded areas indicate the threshold region between 10% and 90% breakdown probabilities. E_{th} (the 50% breakdown probability) lies in the center of the shaded area.

as the aberrations of the optical system increase. This is explainable partly by the higher light transmission through the plasma in the case of aberrations (Fig. 6). However, the conversion into bubble energy is higher for focusing with minimized aberrations even when the bubble energy is related to the *absorbed* laser energy. The absorbed energy can be approximated by $E_{\mathrm{abs}} = E_{\mathrm{in}}(1 - T)$ because light scattering and reflection by the plasma are negligibly small.[10] In the case of strong aberrations $[\Phi(r_G) = 18.5\lambda]$, we thus obtain for $E_{\mathrm{in}} = 1$ mJ a value of $E_B/E_{\mathrm{abs}} = 10\%$, as compared with 21% for focusing with minimized aberrations. The respective values for $E_{\mathrm{in}} = 8$ mJ (the highest energy value for which T was measured) are 13% and 22%. The conversion of absorbed laser energy into cavitation-bubble energy is thus approximately twice as effective with minimized aberrations, as in the case of $\Phi(r_G) = 18.5\lambda$, regardless of the laser-pulse energy. The reason is probably that the average energy density in the plasma is lower in the presence of aberrations caused by the irregular irradiance distribution in the focal region and the longer plasma length. Thus the plasma volume corresponding to a certain amount of absorbed laser energy is larger, hence a larger percentage of the absorbed laser energy is required to evaporate the liquid within the plasma volume. Therefore less energy is available for mechanical effects like shock-wave and bubble generation.

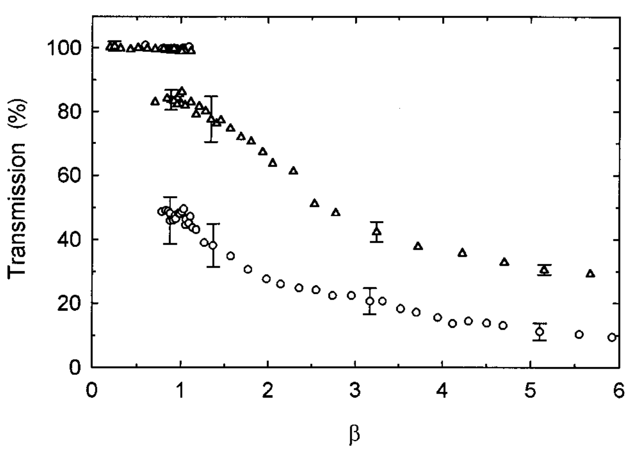

Fig. 6. Transmission as a function of the normalized laser energy $\beta = E/E_{\mathrm{th}}$ for minimized aberrations (open circles) and $\Phi(r_G) = 18.5\lambda$ (open triangles).

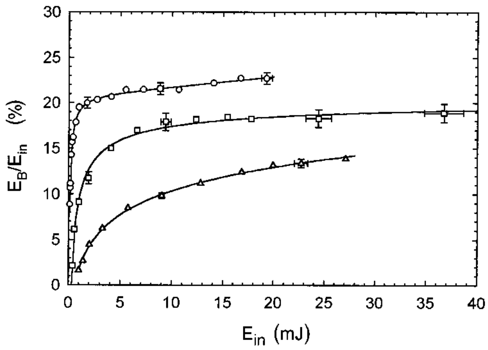

Fig. 7. Conversion rate E_B/E_{in} of the incident light energy E_{in} into cavitation-bubble energy E_B for minimized aberrations (open circles), $\Phi(r_G) = 5.5\lambda$ (open squares), and $\Phi(r_G) = 18.5\lambda$ (open triangles).

The current investigations explain some discrepancies in previous studies on the mechanical effects of optical breakdown in water. In an early paper from our group[39] in which optical breakdown was generated without special attention paid to the minimization of aberrations, the conversion rate of light energy into cavitation-bubble energy was found to be not greater than 8%, but, in later studies in which aberrations were minimized, we observed a conversion rate of as high as 25%,[8,34] although the laser-pulse duration and focusing angle were similar.

F. Consequences for Intraocular Photodisruption

The increase of the optical-breakdown threshold that is due to spherical aberrations demands that higher pulse energies be used for intraocular microsurgery. At the same time, aberrations correlate with an increase in transmission and thus with a reduction of the efficacy of intraocular laser surgery. At equal incident energy the transmitted energy is, by a factor of approximately 20, higher for $\Phi(r_G) = 18.5\lambda$ than for minimized aberrations (Fig. 5). The increased transmission leads to a higher risk of retinal damage. For these reasons it is essential that aberrations be minimized for clinical laser applications. A key element is the appropriate choice and handling of the contact lens used for laser treatment (a contact lens is placed on the corneal surface to immobilize the eye, prevent blinking, adjust the focusing angle, and improve the optical surface that determines the beam quality within the eye.[4,5] Rol *et al.*[30] showed that focusing behind the aplanatic point of a contact lens introduces severe spherical aberrations. It is therefore very important to use different contact lenses for surgical applications in the different segments of the eye.[30] In particular, the use of contact lenses designed for the anterior segment (i.e., for iridotomies and capsulotomies) should be avoided in surgery behind the posterior lens capsule. In clinical practice aberrations may also arise from a tilting of the contact lens and from oblique light passage through the optical media,[4,40] which occurs during treatment in the retinal periphery. Coma and astigmatism have not been investigated in this study but are expected to have deleterious effects similar to those of spherical aberration. They can be minimized by the avoidance of oblique incidence of the laser beam onto the contact lens and oblique light passage through the ocular media.

The authors thank Stefan Rein for his contribution to the early phase of the project and appreciate helpful discussions with Joachim Noack and Daniel X. Hammer. The research was supported by the Deutsche Forschungsgemeinschaft (grant Bi-321/2-3).

References

1. S. J. Gitomer and R. D. Jones, "Laser-produced plasmas in medicine," IEEE Trans. Plasma Sci. **19,** 1209–1219 (1991).
2. A. Vogel, "Nonlinear absorption: intraocular microsurgery and laser lithotripsy," Phys. Med. Biol. **42,** 895–912 (1997).
3. M. R. Prince, G. M. LaMuraglia, P. Teng, T. F. Deutsch, and R. R. Anderson, "Preferential ablation of calcified arterial plaque with laser-induced plasmas," IEEE J. Quantum Electron. **QE-23,** 1783–1786 (1987).
4. R. F. Steinert and C. A. Puliafito, *The Nd:YAG Laser in Ophthalmology* (Saunders, Philadelphia, Pa., 1985).
5. F. Fankhauser and S. Kwasniewska, "Neodymium:yttrium-aluminium-garnet laser," in *Ophthalmic Lasers*, 3rd ed., F. A. L'Esperance, ed. (Mosby, St. Louis, Mo., 1989), pp. 781–886.
6. A. Vogel, P. Schweiger, A. Frieser, M. Asiyo, and R. Birngruber, "Intraocular Nd:YAG laser surgery: light–tissue interaction, damage range, and reduction of collateral effects," IEEE J. Quantum Electron. **26,** 2240–2260 (1990).
7. C. P. Cain, C. D. DiCarlo, B. A. Rockwell, P. K. Kennedy, G. N. Noojin. D. J. Stolarski, D. X. Hammer, C. A. Toth, and W. P. Roach, "Retinal damage and laser-induced breakdown produced by ultrashort-pulse lasers," Graefe's Arch. Clin. Exp. Ophthalmol. **234,** Suppl. 1, S28–S37 (1996).
8. A. Vogel, S. Busch, K. Jungnickel, and R. Birngruber, "Mechanisms of intraocular photodisruption with picosecond and nanosecond laser pulses," Lasers Surg. Med. **15,** 32–43 (1994).
9. A. Vogel, K. Nahen, and D. Theisen, "Plasma formation in water by picosecond and nanosecond Nd:YAG laser pulses. Part I. Optical breakdown at threshold and superthreshold irradiance," IEEE J. Select. Topics Quantum Electron. **2,** 847–860 (1997).
10. K. Nahen and A. Vogel, "Plasma formation in water by picosecond and nanosecond Nd:YAG laser pulses. Part II. Plasma transmission, scattering and reflection," IEEE J. Select. Topics Quantum Electron. **2,** 861–871 (1997).
11. F. W. Campbell and R. W. Gubish, "Optical quality of the human eye," J. Physiol. (London) **186,** 558–578 (1966).
12. W. M. Rosenblum and J. L. Christensen, "Objective and subjective spherical aberration measurement of the human eye," Progr. Opt. **13,** 69–91 (1976).
13. J. Liang, B. Grimm, S. Goelz, and J. Bille, "Objective measurement of wave aberrations of the human eye with the use of a Hartmann–Shack wave-front sensor," J. Opt. Soc. Am. A **11,** 1949–1957 (1994).
14. P. Artal and A. Guirao, "Contributions of the cornea and the lens to the aberrations of the human eye," Opt. Lett. **23,** 1713–1715 (1998).
15. L. D. Santana Haro and J. C. Dainty, "Single-pass measurements of the wave-front aberrations of the human eye by use of retinal lipofuscin autofluorescence," Opt. Lett. **24,** 61–63 (1999).
16. H. P. Loertscher, "Laser-induced breakdown for ophthalmic applications," in *YAG Laser Ophthalmic Microsurgery*, S. C. Trokel, ed. (Appleton-Century-Crofts, Norwalk, Conn., 1983), pp. 39–66.
17. R. F. Steinert and C. A. Puliafito, "Plasma formation and shielding by three ophthalmic neodymium-YAG lasers," Am. J. Ophthalmol. **96,** 427–434 (1983).
18. R. F. Steinert, C. A. Puliafito, and C. Kittrell, "Plasma shielding by *Q*-switched and mode-locked Nd:YAG lasers," Ophthalmology **90,** 1003–1006 (1983).
19. F. Docchio, C. A. Sacchi, and J. Marshall, "Experimental investigation of optical breakdown thresholds in ocular media under single pulse irradiation with different pulse durations," Lasers Ophthalmol. **1,** 83–93 (1986).
20. M. R. C. Capon, F. Docchio, and J. Mellerio, "Nd:YAG laser photodisruption: an experimental investigation on shielding and multiple plasma formation," Graefes Arch. Clin. Exp. Ophthalmol. **226,** 362–366 (1988).
21. F. Docchio and C. A. Sacchi, "Shielding properties of laser-induced plasmas in ocular media irradiated by single Nd:YAG pulses of different durations," Invest. Ophthalmol. Visual Sci. **29,** 437–443 (1988).
22. F. Docchio, "Spatial and temporal dynamics of light attenuation and transmission by plasmas induced in liquids by nanosecond Nd:YAG laser pulses," Nouv. Cimento **13,** 87–98 (1991).
23. S. A. Boppart, C. A. Toth, W. P. Roach, and B. A. Rockwell, "Shielding effectiveness of femtosecond laser-induced plasmas in ultrapure water," in *Laser Tissue Interaction IV*, S. L. Jacques, ed., Proc. SPIE **1882,** 347–354 (1993).
24. D. X. Hammer, R. J. Thomas, G. D. Noojin, B. A. Rockwell, and A. Vogel, "Ultrashort pulse laser induced bubble creation thresholds in ocular media," in *Laser Tissue Interaction VI*, S. L. Jacques, ed., Proc. SPIE **2391,** 30–40 (1995).
25. P. K. Kennedy, S. A. Boppart, D. X. Hammer, B. A. Rockwell, G. D. Noojin, and W. P. Roach, "A first-order model for computation of laser-induced breakdown thresholds in ocular and aqueous media. Part II. Comparison to experiment," IEEE J. Quantum Electron. **31,** 2250–2257 (1995).
26. D. X. Hammer, E. D. Jansen, M. Frenz, G. D. Noojin, R. J. Thomas, J. Noack, A. Vogel, B. A. Rockwell, and A. J. Welch, "Shielding properties of laser-induced breakdown in water for pulse durations from 5 ns to 125 fs," Appl. Opt. **36,** 5630–5640 (1997).
27. L. R. Evans and C. G. Morgan, "Lens aberration effects in optical-frequency breakdown of gases," Phys. Rev. Lett. **22,** 1099–1102 (1969).

28. C. G. Morgan, "Laser-induced breakdown in gases," Rep. Prog. Phys. **38,** 621–665 (1975).
29. W. L. Smith, J. H. Bechtel, and N. Bloembergen, "Dielectric-breakdown threshold and nonlinear-refractive-index measurements with picosecond laser pulses," Phys. Rev. B **12,** 706–714 (1975).
30. P. Rol, F. Fankhauser, and S. Kwasniewska, "Evaluation of contact lenses for laser therapy. Part I," Lasers Ophthalmol. **1,** 1–20 (1986).
31. A. E. Siegman, M. W. Sasnett, and T. F. Johnston, "Choice of clip levels for beam width measurements using knife-edge techniques," IEEE J. Quantum Electron. **27,** 1098–1104 (1991).
32. M. W. Sasnett, "Propagation of multimode laser beams—the M^2 factor," in *The Physics and Technology of Laser Resonators*, D. R. Hall and P. E. Jackson, eds. (Adam Hilger, New York, 1989), pp. 94–105.
33. J. M. Aaron, C. L. M. Ireland, and C. G. Morgan, "Aberration effects in the interaction of focused laser beams with matter," J. Appl. Phys. J. Phys. D **7,** 1907–1917 (1974).
34. A. Vogel, S. Busch, and U. Parlitz, "Shock wave emission and cavitation bubble generation by picosecond and nanosecond optical breakdown in water," J. Acoust. Soc. Am. **100,** 148–165 (1996).
35. A. Vogel, W. Hentschel, J. Holzfuss, and W. Lauterborn, "Cavitation bubble dynamics and acoustic transient generation in ocular surgery with pulsed neodymium:YAG lasers," Ophthalmology **93,** 1259–1269 (1986).
36. J. W. Rayleigh, "On the pressure developed in a liquid during the collapse of a spherical cavity," Philos. Mag. **34,** 94–98 (1917).
37. A. Vogel, J. Noack, K. Nahen, D. Theisen, S. Busch, U. Parlitz, D. X. Hammer, G. D. Noojin, B. A. Rockwell, and R. Birngruber, "Energy balance of optical breakdown in water at nanosecond to femtosecond time scales," Appl. Phys. B. **68,** 271–280 (1999).
38. F. Docchio, P. Regondi, M. R. C. Capone, and J. Mellerio, "Study of the temporal and spatial dynamics of plasmas induced in liquids by nanosecond Nd:YAG laser pulses. 1: analysis of the plasma starting times," Appl. Opt. **27,** 3661–3668 (1988).
39. A. Vogel and W. Lauterborn, "Acoustic transient generation by laser-produced cavitation bubbles near solid boundaries," J. Acoust. Soc. Am. **84,** 719–731 (1988).
40. F. Fankhauser, U. Dürr, H. Giger, P. Rol, and S. Kwasniewska, "Lasers, optical systems and safety in ophthalmology: a review," Graefes Arch. Clin. Exp. Ophthalmol. **234,** 473–487 (1996).